Hindawi
Journal of Advanced Transportation
Volume 2020, Article ID 8819911, 15 pages
https://doi.org/10.1155/2020/8819911

Research Article

Multilane Spatiotemporal Trajectory Optimization Method (MSTTOM) for Connected Vehicles

Pangwei Wang,[1] **Yunfeng Wang**,[1] **Hui Deng**,[1] **Mingfang Zhang**,[1] **and Juan Zhang**[2]

[1]*Beijing Key Lab of Urban Intelligent Traffic Control Technology, North China University of Technology, Beijing 100144, China*
[2]*College of Engineering, Mathematics and Physical Sciences, University of Exeter, EX4 4QF, Exeter, UK*

Correspondence should be addressed to Juan Zhang; jz397@exeter.ac.uk

Received 30 September 2020; Revised 17 November 2020; Accepted 27 November 2020; Published 15 December 2020

Academic Editor: Xiaolei Ma

It is agreed that connected vehicle technologies have broad implications to traffic management systems. In order to alleviate urban congestion and improve road capacity, this paper proposes a multilane spatiotemporal trajectory optimization method (MSTTOM) to reach full potential of connected vehicles by considering vehicular safety, traffic capacity, fuel efficiency, and driver comfort. In this MSTTOM, the dynamic characteristics of connected vehicles, the vehicular state vector, the optimized objective function, and the constraints are formulated. The method for solving the trajectory problem is optimized based on Pontryagin's maximum principle and reinforcement learning (RL). A typical scenario of intersection with a one-way 4-lane section is measured, and the data within 24 hours are collected for tests. The results demonstrate that the proposed method can optimize the traffic flow by enhancing vehicle fuel efficiency by 32% and reducing pollutants emissions by 17% compared with the advanced glidepath prototype application (GPPA) scheme.

1. Introduction

The traffic capacity of urban road network is restricted by the time delay, potential safety hazards, and environmental pollution caused by traffic congestion. According to the US Department of Transportation Statistics issued in 2019, 27% of highways in the United States are blocked at the peak of urban traffic and 54% of vehicles are in the state of congestion [1]. Intersections, as important nodes of urban road network, cause 80% of these urban traffic congestions [2]. Therefore, alleviating urban traffic congestion by taking the intersection as the optimization object is a challenging work.

The realization of spatiotemporal trajectory optimization mainly includes two parts: (1) realizing the dynamic speed control of multiple vehicles in the longitudinal direction; (2) achieving the cooperative lane-changing control of multiple vehicles in the horizontal direction. In the intelligent traffic system (ITS) strategic plan published by the US Department of Transportation in 2010, dynamic speed coordination based on spatiotemporal trajectory was denoted as one of the important methods for traffic flow optimization of road network [3]. Grumert and Tapani [4] established a variable speed limit (VSL) algorithm based on the traffic occupancy. The results show that VSL can increase traffic flow by 16%. Jo et al. [5] updated a VSL algorithm by detecting vehicles at multiple stations from the perspective of road safety, which solved the guidance delay problem. With the development of cooperative vehicle infrastructure system (CVIS) and connected vehicles (CVs), the problem of discontinuous dynamic speed limit can be solved by continuous dynamic speed control [6]. Considering the random traffic conditions, Zhu and Ukkusuri [7] proposed a method to realize dynamic speed limit control through RL. In this method, a link based dynamic network load model was established in the environment of CVs, which can reduce the total travel time by 18%. Aldana-Muñoz et al. [8] proposed a method by combining environmental driving and speed guidance to optimize the continuous linear spatiotemporal trajectory. The experimental results show that the linear spatiotemporal trajectory optimization can stabilize the change of

disturbance on traffic flow. Wang et al. [9] proposed a speed guidance model based on model predictive control (MPC), by which the spatiotemporal trajectory can be constructed in advance. Wei et al. [10] proposed a cooperative optimization method for multivehicle spatiotemporal trajectories, which is established based on the simplified Newell linear car-following model. Considering different road environments and weather conditions, De Mello and Chiodi [11] proposed a fuzzy logic control model of spatiotemporal trajectory, which increases the effectiveness of decision-making process by 13%. Liang et al. [12] presented a method to optimize the common spatiotemporal trajectories for both autonomous vehicles and manual driving vehicles. With the proportion of autonomous vehicles increasing, average delay time is reduced by 25% and average stopping time is reduced by 47%. Wang et al. [13, 14] designed a joint control model for CVs and traffic signal, which aims to optimize vehicular platoon and signal timing to improve traffic efficiency at intersections. The simulation results show that the joint control model can reduce the stopping time by 54%. Mirheli et al. [15] proposed a distributed cooperative control logic based on spatiotemporal trajectory, which can be applied to unsignalized intersections. In this study, vehicles with this logic application scheme can pass through the unsignalized intersection in optimal trajectories without collision. Wang et al. [16] developed a cooperative optimization method of spatiotemporal trajectory with multiple intersection phases. In this method, a lower bound estimator based on dynamic load network was constructed to improve robustness and stability of vehicle dynamic network.

Urban roads or expressways with single lane or dual lane were mainly taken in the above studies; however, the multilane spatiotemporal trajectory optimization is still lacked in the research. The main challenge of vehicles in the multilane spatiotemporal trajectory lies in how to solve its complex lane-changing problem. Moreover, accidents caused by lane-changing behaviors make the multiple lanes occupied, which makes the road congestion more serious [17]. Considering the risk of lane-changing produced by vehicle-to-vehicle (V2V) communication delay, Hongil and Jae-Il [18] proposed an oriented bounding box (OBB) method which reduces communication delay by defining the lateral and longitudinal gradient controllers. Li et al. [19] proposed a new lane-changing model based on CVs to evaluate the critical vehicle distance in lane-changing process. The safety potential field theory was integrated, and the vehicle movement state under different speed and acceleration conditions is dynamically presented. Finally, the lane-changing route can be determined through the selection of spatiotemporal trajectory. The majority of studies provide ideas and theoretical support for multivehicle cooperative lane-changing based on spatiotemporal trajectory. However, due to the massive amount of data calculation and high system complexity in multilane spatiotemporal trajectories, the common multilane road section traffic efficiency problem has not been effectively solved and improved through the optimization of multiple single lanes method.

To solve the above problems, MSTTOM for connected vehicles is established in this paper. The spatial temporal trajectories are generated and combined with vehicular current state information and the signal timing information. In addition, during the driving process, the trajectories can be optimized by RL. Moreover, the vehicle can change the lane and update its trajectory through the cooperative lane-changing strategy designed in this model. The significant contribution of this research is that vehicles can pass through intersections in optimal spatiotemporal trajectory and further solve the congestion problem in current multilane road section.

The rest of this paper is organized as follows: The typical application scenario and the structure of the method are introduced in Section 2. The specific content of MSTTOM is described in Section 3, where the trajectory is generated and optimized. The simulation experiment results through SUMO/Python are presented and analyzed in Section 4, and the stability of headway, fuel consumption rate, pollutant emission, and calculation time are also selected as the evaluation indexes. Finally, Section 5 concludes the paper.

2. Typical Application Scenario for Connected Vehicles

2.1. Application Scenario. The upstream section of the intersection, as the application of multilane scenario, is covered by vehicle-to-everything (V2X) wireless communication and shown in Figure 1. The vehicular trajectory from upstream to intersection process will be dynamically calculated based on MSTTOM.

2.2. System Structure. The flow chart of MSTTOM is shown in Figure 2. The procedure can be described as follows: the traffic signal and vehicular driving information is collected firstly by road-side unit (RSU) and on-board unit (OBU), so that the target lane and arrival time at current intersection can be calculated; secondly, the optimal trajectory is generated through connected vehicular state and constraints, where traffic capacity of current intersection can be optimized online through the cooperative lane-changing strategy; and finally, every connected vehicle can pass through the intersection with least travel time through the optimization result of RL. The spatiotemporal trajectory and the optimized state are clarified in Figure 3.

3. Multilane Spatiotemporal Trajectory Optimization Method (MSTTOM)

Firstly, state vectors defined in this paper contain the information of vehicular driving, such as position, speed, and acceleration, and the information of traffic signal timing. Secondly, the cost function and constraints of vehicular trajectory are formulated. Finally, the optimal vehicular trajectory is dynamically calculated through maximum principle and RL.

3.1. State Vector. In the typical scenario of urban intersection, we define the vehicle entering the road section as C_{mn}, where m and n represent the m-th lane of the road section

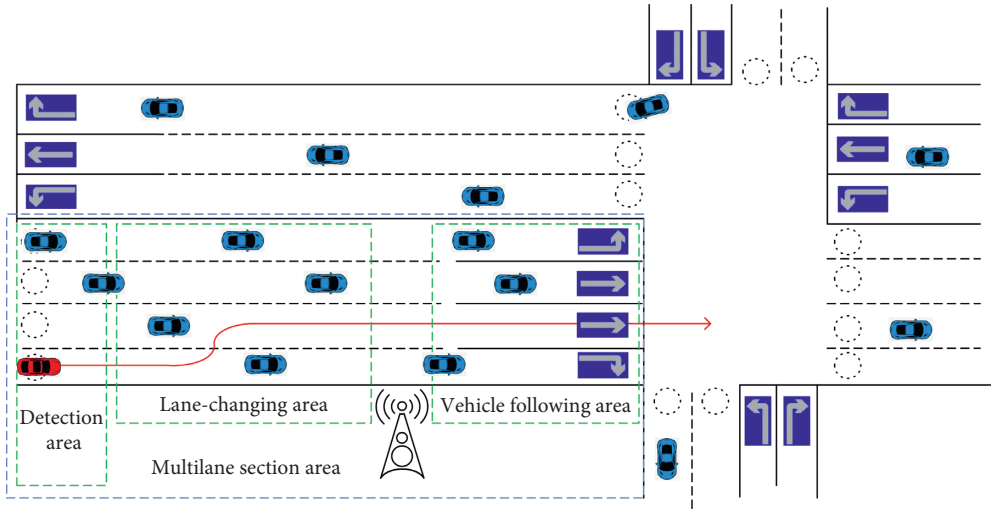

Figure 1: The scenario of multilane section based on connected vehicles.

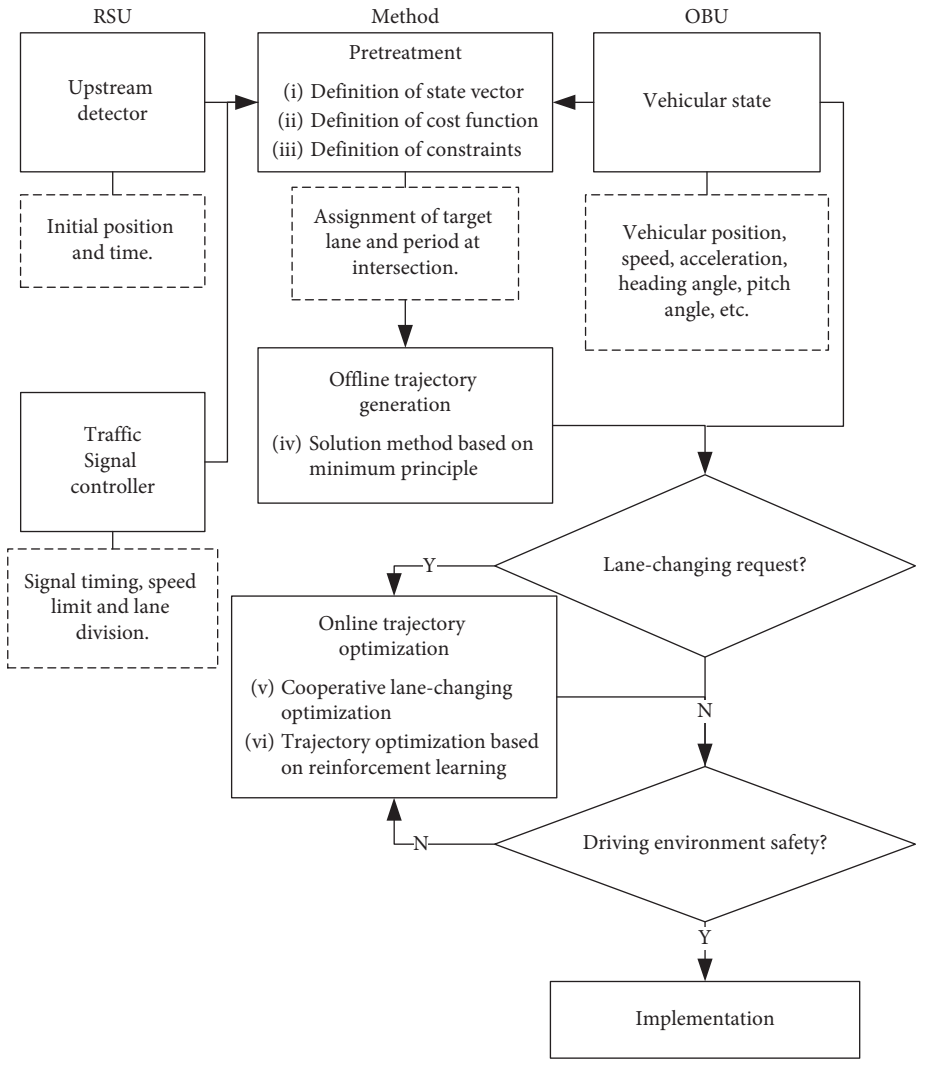

Figure 2: The flow chart of spatiotemporal trajectory optimization process for connected vehicles.

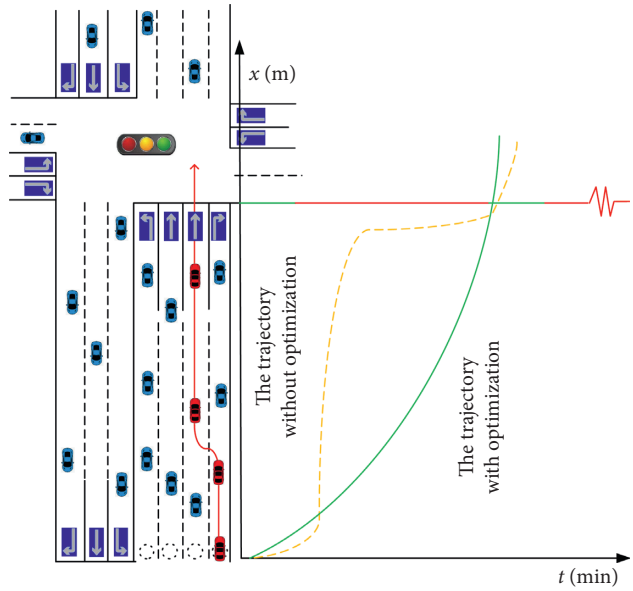

Figure 3: The spatiotemporal trajectory with and without optimization.

from the right side to the left side (the target vehicle is selected as the reference) and the n-th vehicle from the downstream to the upstream, respectively. Therefore, we define the state vector of vehicle C_{mn} as $\boldsymbol{x}_{mn}(t)$:

$$\mathbf{x}_{mn}(t) = \left[x_{mn}(t), y_{mn}(t), v_{mn}(t), v_{mn}'(t)\right]^T, \tag{1}$$

where $(x_{mn}(t), y_{mn}(t))$ is the position of vehicle C_{mn} at time t, $v_{mn}(t)$ is the driving speed of vehicle C_{mn} at time t, and $v'_{mn}(t)$ is the lateral speed of vehicle C_{mn} at time t.

The method input is the vehicle acceleration $\boldsymbol{u}_{mn}(t)$, which can be expressed as follows:

$$\mathbf{u}_{mn}(t) = \left[u_{mn}(t), u_{mn}'(t)\right]^T, \tag{2}$$

where $u_{mn}(t)$ is the longitudinal acceleration of vehicle C_{mn} at time t and $u'_{mn}(t)$ is the current lateral acceleration of vehicle C_{mn} at time t.

Meanwhile, the signal timing information of vehicle target lane $\varphi_{mn}(t)$ and the traffic flow information I_{m-1} and $I_{m-1}(t)$ of adjacent lanes $m+1$ and $m-1$ are defined as

$$\begin{aligned} \boldsymbol{\varphi}_{mn}(t) &= \left[\varphi_{mn}(t), t_{\varphi_{mn}(t)}, R_m, G_m\right], \\ \mathbf{I}_{m+1}(t) &= \left[k_{m+1}(t)\right], \\ \mathbf{I}_{m-1}(t) &= \left[\overline{v}_{m+1}(t), k_{m-1}(t)\right], \end{aligned} \tag{3}$$

where $\varphi_{mn}(t)$ is the target phase state of vehicle C_{mn}, $t_{\varphi_{mn}(t)}$ is the remaining time of phase $\varphi_{mn}(t)$, R_m is the red light duration of lane m, G_m is the green light duration of lane m, $\overline{v}_{m+1}(t)$ and $\overline{v}_{m-1}(t)$ stand for the average traffic flow velocity of left lane $m+1$ and right lane m-1, and k_{m+1} and k_{m-1} are the average traffic flow density of left lane $m+1$ and right lane $m-1$. The average traffic flow speed $\overline{v}_m(t)$ and average traffic flow density $k_m(t)$ can be expressed as

$$\begin{aligned} \overline{v}_m(t) &= \frac{\sum_{N=N_m^{\min}}^{N_m^{\max}} mN}{N_m^{\max} - N_m^{\min} + 1}, \\ k_m(t) &= \frac{N_m^{\max} - N_m^{\min} + 1}{L}, \end{aligned} \tag{4}$$

where N is the total number of vehicles, $N_m^{\max}$ is the maximum number of vehicles in lane m, $N_m^{\min}$ is the minimum number of vehicles in lane m, and L is the length of road section.

The system state equation is described as

$$\dot{x}_{mn}(t) = f\left(\mathbf{x}_{mn}(t), \mathbf{u}_{mn}(t), \boldsymbol{\varphi}_{mn}(t), \mathbf{I}_{m+1}(t), \mathbf{I}_{m-1}(t)\right). \tag{5}$$

3.2. Cost Function. In order to ensure that the vehicle can accurately follow the designed trajectory of the system, fixed and variable costs in the process from upstream to downstream are considered and formulated, which can be represented by

$$J = g\left(\mathbf{x}_{mn}\left(t_{mn}^{\text{out}}\right)\right) + \int_{t_{mn}^0}^{t_{mn}^{\text{out}}} h\left(\mathbf{x}_{mn}(t), \mathbf{u}_{mn}(t)\right)\mathrm{d}t, \tag{6}$$

where t_{mn}^{out} is the time when vehicle C_{mn} leaves the road section, t_{mn}^0 is the time when the vehicle C_{mn} enters the road section, $g(\mathbf{x}_{mn}(t_{mn}^{\text{out}}))$ is the fixed cost of the process, and $\int_{t_{mn}^0}^{t_{mn}^{\text{out}}} h(\mathbf{x}_{mn}(t), \mathbf{u}_{mn}(t))\mathrm{d}t$ is the variable cost of the process. The fixed cost includes the cost of fixed items (such as the driving distance and expected speed at the intersection) and the travel time of the road section. The process can be described as

$$g\left(x_{mn}\left(t_{mn}^{\text{out}}\right)\right) = w_1\left(t_{mn}^{\text{out}} - \overline{t}_{mn}^{\text{out}}\right)^2 + w_2\left(x_{mn}\left(t_{mn}^{\text{out}}\right) - L\right)^2 + w_3\left(v_{mn}\left(t_{mn}^{\text{out}}\right) - \overline{v}_{mn}^{\text{out}}\right)^2 + w_4\left(y_{mn}\left(t_{mn}^{\text{out}}\right) - \mathrm{d}\left(\overline{t}_{mn}^{\text{out}}\overline{m} - \frac{1}{2}\right)\right)^2, \tag{7}$$

where $\overline{t}_{mn}^{\text{out}}$ is the target time of vehicle C_{mn} driving out of the road section, $\overline{v}_{mn}^{\text{out}}$ is the expected speed of vehicle C_{mn} at the intersection, $\overline{m}$ is the target lane of vehicle, and d is the lane width. w_1, w_2, w_3, w_4 are the weights of the travel time of the road section, driving length of the road section, expected speed at the intersection, and the target lane at the intersection, respectively. $w_1, w_2, w_3, w_4 \in R+$.

Variable cost involves acceleration and deceleration of the vehicle driving in longitudinal and lateral lanes. Its function can be expressed as

$$h\left(\mathbf{x}_{mn}(t), \mathbf{u}_{mn}(t)\right) = w_5\left(u_{mn}(t)^2 + 2u_{mn}(t)v_{mn}(t)\right)\chi\left(u_{mn}(t)\right) + w_6\left(u_{mn}'(t)^2 + 2u_{mn}'(t)v_{mn}'(t)\right), \tag{8}$$

where w_5 and w_6 are the weights of energy changes caused by longitudinal and lateral acceleration of the vehicle, receptively. w_5, $w_6 \in R+$. $\chi(u_{mn}(t))$ is the Heaviside function of longitudinal acceleration of networked vehicles and can be used to separate the variable cost induced by acceleration in longitudinal deceleration process:

$$\chi\left(u_{mn}(t)\right) = \begin{cases} 0, u_{mn}(t) \le 0, \\ 1, u_{mn}(t) > 0. \end{cases} \tag{9}$$

$\overline{t}_{mn}^{\text{free}}$ denotes the time of vehicles passing through the intersection under the condition of low-density traffic flow, also known as the time for vehicles C_{mn} leaving the road without restriction. The time consists of four parts: initial time t_{mn}^0, time t_{mn}^{acc} at acceleration state, time $t_{mn}^{c.s.}$ at constant speed state, and time t_{mn}^{dec} at deceleration state, which can be described as follows:

$$\overline{t}_{mn}^{\text{free}} = t_{mn}^0 + t_{mn}^{acc} + t_{mn}^{c.s.} + t_{mn}^{dec}, \tag{10}$$

where t_{mn}^{acc}, $t_{mn}^{c.s.}$, and t_{mn}^{dec} can be expressed as

$$\begin{aligned} t_{mn}^{acc} &= \frac{v_0^{\lim} - v_{mn}\left(t_{mn}^0\right)}{u_{mn}^{+\max}}, \\ t_{mn}^{c.s.} &= \frac{L - \left(\left(\left(v_0^{\lim}\right)^2 - v_{mn}\left(t_{mn}^0\right)^2\right)/2u_{mn}^{+\max}\right) - \left(\left(\left(v_0^{\lim}\right)^2 - \left(v_m^{\lim}\right)^2\right)/2u_{mn}^{-\max}\right)}{v_0^{\lim}}, \\ t_{mn}^{dec} &= \frac{v_0^{\lim} - v_m^{\lim}}{u_{mn}^{-\max}}, \end{aligned} \tag{11}$$

where $v_0^{\lim}$ is the speed limit of the road section, $v_m^{\lim}$ is the speed limit at the downstream exit of the lane m, $u_{mn}^{+\max}$ is the maximum acceleration of vehicle C_{mn}, and $u_{mn}^{-\max}$ is the maximum deceleration of vehicle C_{mn}.

However, it is impossible for the urban road section to maintain a low-density state. Therefore, connected vehicles have to pass through current intersection as a temporary platoon. The candidate time $\overline{t}_{mn}^{\text{temp}}$ of vehicle C_{mn} can be calculated as

$$\overline{t}_{mn}^{\text{temp}} = \max\left(\overline{t}_{m(n-1)}^{\text{out}} + t_m^{h2h}, \overline{t}_{mn}^{\text{free}}\right), \tag{12}$$

where t_m^{h2h} is the minimum headway between two adjacent vehicles in lane m at the downstream exit of the section.

In order to improve the traffic capacity of intersections, the target time $\overline{t}_{mn}^{\text{out}}$ of vehicle C_{mn} at current intersection is controlled within the passable green signal, which can be selected according to

$$\overline{t}_{mn}^{\text{out}}, = \begin{cases} \overline{t}_{mn}^{\text{temp}}, \overline{t}_{mn}^{\text{temp}} \in \xi_m, \\ floor\left(\dfrac{\overline{t}_{mn}^{\text{temp}}}{R_m + G_m}\right)\left(R_m + G_m\right) + R_m, \overline{t}_{mn}^{\text{temp}}, \notin \xi_m, \end{cases} \tag{13}$$

where ξ_m is the set of green light periods of lane m, and *floor* (t) is the function of rounding down.

The expected speed of vehicles is defined as the speed limit at the downstream exit to ensure the maximum efficiency of vehicles and can be described as

$$\overline{v}_{mn}^{\text{out}} = v_m^{\lim}. \tag{14}$$

In conclusion, the cost function can be integrated as

$$J = w_1\left(t_{mn}^{\text{out}} - \overline{t}_{mn}^{\text{out}}\right)^2 + w_2\left(x_{mn}\left(t_{mn}^{\text{out}}\right) - L\right)^2 + w_3\left(v_{mn}\left(t_{mn}^{\text{out}}\right) - \overline{v}_{mn}^{\text{out}}\right)^2 + w_4\left(y_{mn}\left(t_{mn}^{\text{out}}\right) - d\left(\overline{m} - \frac{1}{2}\right)\right)^2 + \int_{t_{mn}^0}^{t_{mn}^{\text{out}}}\left(w_5\left(u_{mn}(t)^2 + 2u_{mn}(t)v_{mn}(t)\right)\chi\left(u_{mn}(t)\right) + w_6\left(u_{mn}'(t)^2 + 2u_{mn}'(t)v_{mn}'(t)\right)\right)\mathrm{d}t. \tag{15}$$

3.3. Constraints. In order to minimize the above cost function J, seven constraints, namely, initial vehicular state, vehicle spacing, speed, acceleration, jerk, signal timing, and wireless communication, should be satisfied in the optimization problem.

3.3.1. Initial Vehicular State. Suppose that a connected vehicle C_{mn} enters the road section with detectors; when $n \geq n_{\max}$, the counter will reset. The initial state of vehicle C_{mn} is defined as

$$\mathbf{x}_{mn}\left(t_{mn}^0\right) = \begin{pmatrix} x_{mn}\left(t_{mn}^0\right) \\ y_{mn}\left(t_{mn}^0\right) \\ v_{mn}\left(t_{mn}^0\right) \\ v_{mn}{}'\left(t_{mn}^0\right) \end{pmatrix} = \begin{pmatrix} 0 \\ \mathrm{d}\left(m - \frac{1}{2}\right) \\ v_{mn}^0 \\ v_{mn}^{0'} \end{pmatrix}. \tag{16}$$

3.3.2. Vehicle Spacing. The vehicle will inevitably be in the vehicle-following state in the driving process. Therefore, vehicle C_{mn} on the lane m and the front vehicle $C_{m\,(n-1)}$ should ensure a certain displacement in space and time. The safety constraint can be formulated as

$$x_{mn}\left(t + \tau_{mn}\right) \leq x_{m(n-1)}(t) - d_{mn}, \tag{17}$$

where τ_{mn} is the time displacement of vehicle C_{mn} and the front vehicle $C_{m\,(n-1)}$, and d_{mn} is the spatial displacement of vehicle C_{mn} and the front vehicle $C_{m\,(n-1)}$.

3.3.3. Speed. In order to ensure the safety of the vehicles in the road section, the speed constraint is applied to them. The longitudinal speed constraint embraces the speed information involving speed limit within the section and the minimum speed 0. Thus, we have

$$0 \leq v_{mn}(t) \leq v_0^{\lim}. \tag{18}$$

For the lateral speed constraint, the vehicle deflection angle is mainly constrained by vehicle dynamics, which can be expressed as

$$\alpha_{-\max} \leq \alpha_{mn}(t) \leq \alpha_{\max}, \tag{19}$$

where $\alpha_{\max}$ is the maximum angle through which the front wheel of the vehicle can turn to the left, $\alpha_{mn}(t)$ represents the steering angle of the front wheel of the current vehicle, and $\alpha_{\max}$ represents the maximum angle through which the front wheel of the vehicle can turn to the right.

Therefore, the lateral restraint condition of the vehicle is shown as

$$v_0^{\lim}\alpha_{-\max} \leq v_{mn}'(t) \leq v_0^{\lim}\alpha_{\max}. \tag{20}$$

3.3.4. Acceleration. In order to guarantee that the engine can provide enough power and the brake pads can provide the vehicle enough power limit, the acceleration or deceleration of the vehicle should be specified as a constraint. The acceleration constraints can be expressed as

$$\begin{cases} u_{-\max} \leq u_{mn}(t) \leq u_{\max}, \\ u_{-\max}' \leq u_{mn}'(t) \leq u_{\max}', \end{cases} \tag{21}$$

where $u_{\max}$ is the acceleration of the maximum longitudinal braking deceleration of the vehicle, $u_{\max}$ is the acceleration of the maximum longitudinal acceleration of the vehicle, $u'_{\max}$ is the maximum transverse acceleration of the vehicle to the left, and $u'_{\max}$ is the maximum acceleration of the vehicle to the right.

3.3.5. Jerk. The jerk constraint is the change rate constraint of vehicle acceleration, also known as the impact constraint or comfort constraint. The purpose of jerk constraint is to eliminate the negative impact of the acceleration change in the driving process. The jerk constraint is shown as

$$\begin{cases} j_{-\max} \leq \dfrac{\partial u_{mn}(t)}{\partial t} \leq j_{\max}, \\ j_{-\max}{}' \leq \dfrac{\partial u_{mn}{}'(t)}{\partial t} \leq j_{\max}{}', \end{cases} \tag{22}$$

where $j_{\max}$ represents the maximum longitudinal backward jerk, $j_{\max}$ represents the maximum longitudinal forward jerk, $j'_{\max}$ represents the maximum lateral left acceleration, and $j'_{\max}$ represents the maximum lateral right acceleration.

3.3.6. Signal Timing. The signal timing constraint of vehicles can ensure that vehicles avoid violations when passing through the intersection, which can be represented as

$$v_{mn}\left(t_{mn}^{\text{out}}\right) = 0, \quad t_{mn}^{\text{out}} \notin \xi_m. \tag{23}$$

3.3.7. Wireless Communication. V2X is a communication system through which a vehicle communicates with any entity that may affect the vehicle. Thus, the essence of V2X

technology is wireless communication technology. In the practical application of wireless communication technology, time delay and packet loss are inevitable, which may affect the stability and security of networked vehicles in the system. The relevant parameters of wireless communication are constrained as follows:

$$\begin{aligned} \widetilde{\tau}_{mn}(t) &< 0.1, \\ P_{lp|mn}(t) &< 15\%, \end{aligned} \tag{24}$$

where $\widetilde{\tau}_{mn}(t)$ and $P_{lp|mn}(t)$ represent the time delay and the packet loss probability of the vehicle C_{mn} at time t.

3.4. Solution Method Based on Maximum Principle. MSTTOM is solved by Pontryagin's maximum principle, and the Hamilton function of the problem is established as

$$H(\mathbf{x}, \mathbf{u}, \boldsymbol{\lambda}, t) = \boldsymbol{\lambda}^T f(\mathbf{x}, \mathbf{u}, t) + h(\mathbf{x}, \mathbf{u}, t), \tag{25}$$

where $\boldsymbol{\lambda}$ is defined as the costate vector of vector $\boldsymbol{x}$, which represents the additional cost of the change of J caused by the small change ∂x of vector $\boldsymbol{x}$.

In the admissible set U, the minimum input $\mathbf{u}^*$ of the cost must satisfy the minimum state of the Hamilton function, which can be expressed as follows:

$$H(\mathbf{x}*, \mathbf{u}*, \boldsymbol{\lambda}*, t) \le H(\mathbf{x}*, \mathbf{u}, \boldsymbol{\lambda}*, t), \forall \mathbf{u} \in U,\ t \in \left[t_{mn}^0, t_{mn}^{\text{out}}\right],$$

$$\begin{cases} \dfrac{\partial H}{\partial u} = 0, \\ \dfrac{\partial H}{\partial x} = -\dot{\lambda}, \\ \dfrac{\partial H}{\partial \lambda} = \dot{x}. \end{cases} \tag{26}$$

Therefore, the Hamilton function of MSTTOM is shown as

$$\begin{aligned} H_{mn} = {} & \lambda_1 v_{mn}(t) + \lambda_2 u_{mn}(t) + w_5 \\ & \left(u_{mn}(t)^2 + 2u_{mn}(t)v_{mn}(t)\right)\chi\left(u_{mn}(t)\right), \end{aligned} \tag{27}$$

where the variation of the lateral movement trajectory is optimized in the process of vehicular cooperative lane-changing.

In the process of solving the problem, the state vector λ should meet the condition of the fixed cost, which is shown as

$$\lambda\left(t_{mn}^{\text{out}}\right) = \frac{\partial g\left(x_{mn}\left(t_{mn}^{\text{out}}\right)\right)}{\partial x_{mn}} \Rightarrow \begin{cases} \lambda_1\left(t_{mn}^{\text{out}}\right) = 2w_2\left(x_{mn}\left(t_{mn}^{\text{out}}\right) - L\right) \\ \lambda_2\left(t_{mn}^{\text{out}}\right) = 2w_3\left(v_{mn}\left(t_{mn}^{\text{out}}\right) - \overline{v}_{mn}^{\text{out}}\right) \end{cases} \tag{28}$$

3.5. Cooperative Lane-Changing Optimization. In order to accurately describe the process of cooperative lane-changing strategy, the request of the vehicular lane-changing is displayed in Figure 4. The vehicle C_{mn}, selected as the subject vehicle, is a red one in the middle of lane m and ready to change lanes from the current lane m to the target lane $m+1$. Besides, yellow vehicles are defined as the primary threat vehicles of C_{mn}, orange vehicles are defined as the secondary threat vehicles of C_{mn}, and blue vehicles are defined as the non-threat vehicles of C_{mn}.

If target lane is not the adjacent lane, it can be decomposed into multiple lane-changing processes. The optimal trajectory is loaded into the traffic environment, and the potential lane-changing conflict safety inspection can be carried out. The flow chart of lane-changing safety inspection is shown in Figure 5.

If two adjacent vehicles receive the same requests concurrently, there is a priority for the vehicle with a higher speed. If adjacent vehicles based on daily driving habits have similar speed, there is a priority for the vehicle in the left lane.

Different traffic saturation should be satisfied in the cooperative lane-changing strategy. The higher the saturation involved in the case is, the higher the complexity of the lane-changing strategy will be supposed. Therefore, the case of higher saturation is discussed as follows:

(i) The subject vehicle C_{mn} initiates a lane-changing request to the target vehicle $C_{(m+1)n}$ after the target gap selected.

(ii) The target vehicle $C_{(m+1)n}$ and its rear vehicle $C_{(m+1)(n+1)}$ adjust their speeds to confirm a safe gap for vehicle C_{mn}.

(iii) Vehicle C_{mn} drives into the target lane $m+1$.

(iv) The spatiotemporal trajectories of vehicles in the original lane and target lane are updated, which is shown in Figure 6.

3.6. Trajectory Optimization Based on RL. In order to improve the efficiency of MSTTOM, this paper designs an optimization algorithm based on the RL paradigm, which can quickly match the optimal trajectory. The optimization algorithm is formulated with the current position and speed of vehicles. The target lane and time period are modeled as inputs, and the sets of vehicle acceleration are formulated as outputs. When the lane-changing request is initiated, the vehicle can be connected to the trajectory of the cooperative lane-changing strategy through the RL matching network. Once the lane-changing is completed, the spatiotemporal trajectory will be matched by the RL to achieve the multilane trajectory optimization.

The state vector of MSTTOM satisfies Markov property; that is, the next state $\boldsymbol{s}_{t+1}$ of the system is only related to the current state $\boldsymbol{s}_t$, but not directly related to the preceding state. Thus, the state vector can be shown as follows:

$$\begin{aligned} s_t &= \left[\mathbf{x}_{mn}(t), \boldsymbol{\varphi}_{mn}(t), \mathbf{I}_{m+1}(t), \mathbf{I}_{m-1}(t)\right], \\ P\left[\mathbf{s}_{t+1}|\mathbf{s}_t\right] &= P\left[\mathbf{s}_{t+1}|\mathbf{s}_1, \mathbf{s}_2, \mathbf{s}_3, \ldots, \mathbf{s}_t\right], \end{aligned} \tag{29}$$

where P is the probability matrix of transition between state.

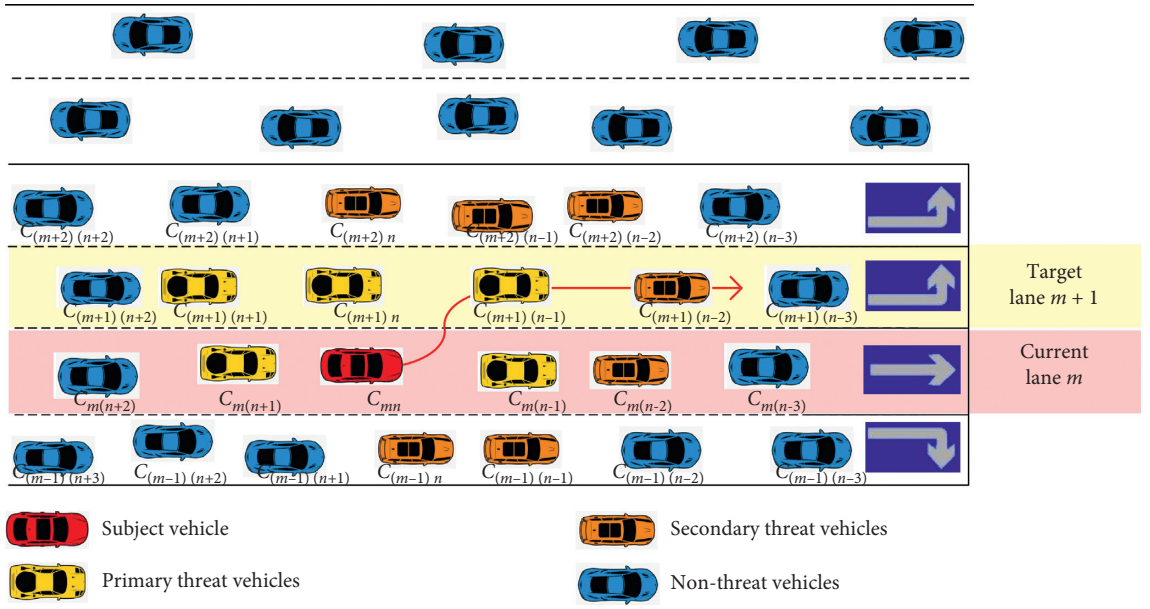

Figure 4: Schematic chart of lane-changing environment for vehicles C_{mn}.

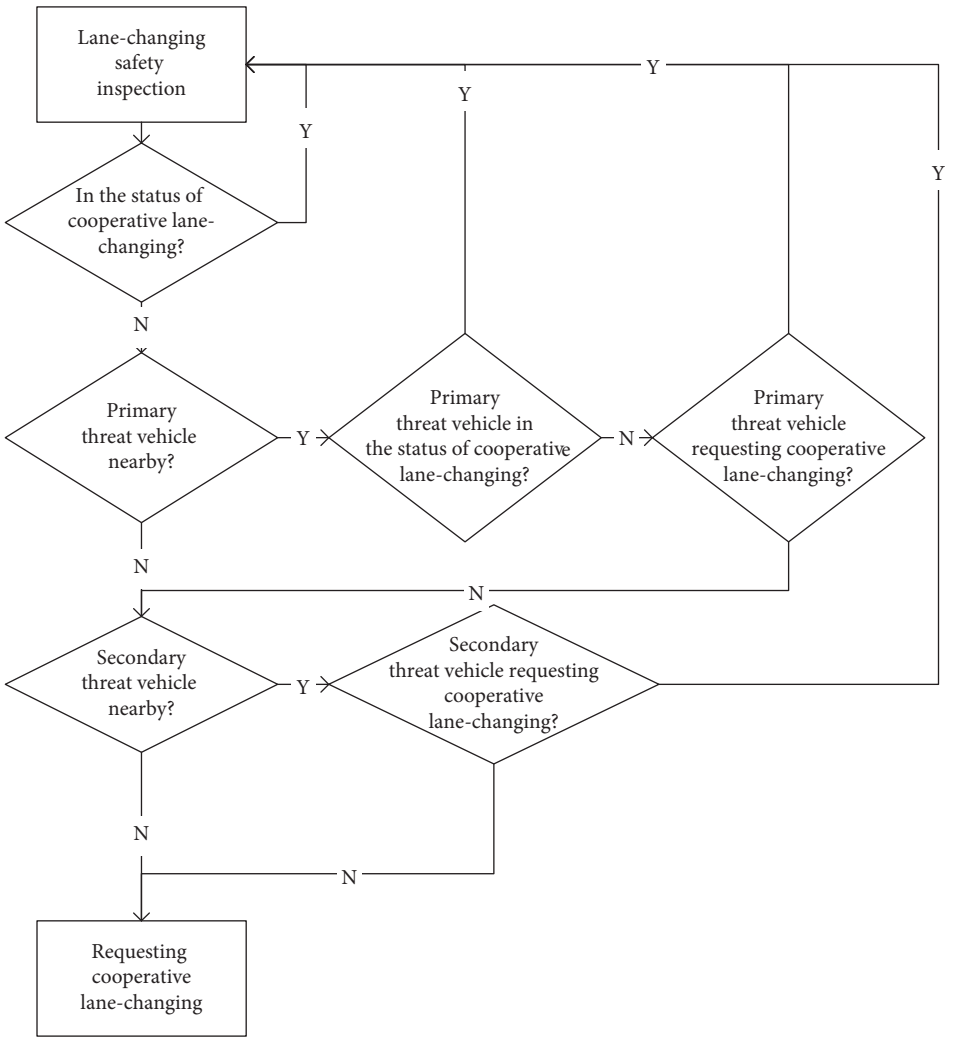

Figure 5: The flow chart of lane-changing safety inspection.

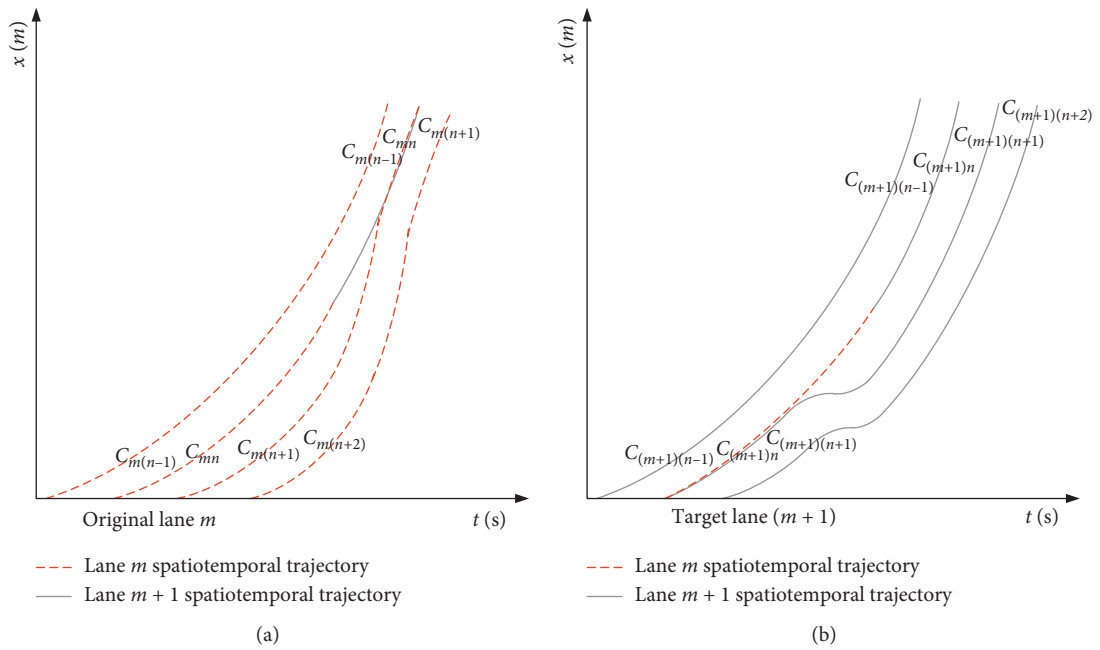

Figure 6: Vehicular spatiotemporal trajectories in lane-changing process.

Through integration, the set of action vectors will be presented in the form of trajectory data. The action vector $\boldsymbol{a}_t$ at current state $\boldsymbol{s}_t$ is shown as

$$\mathbf{a}_t = [\mathbf{u}_{mn}(t)]. \tag{30}$$

Five tuples (S, A, P, R, γ) are defined to describe the process of MSTTOM. Among them, S is the state set, which includes the current state of vehicles and the traffic flow state in the road section; A is the set of executing actions, that is, the set of lateral and longitudinal acceleration output by optimization; R is the reward function of the process, which is negatively linear with the cost function J; and γ is the discount factor when calculating the value function. For a fixed policy π, the value function $v_\pi(\mathbf{s})$ can be calculated as

$$v_\pi(\mathbf{s}) = E_\pi\left[\sum_{k=0}^{\infty} \gamma^k R_{t+k+1} | S_t = s\right]. \tag{31}$$

An action value function $q_\pi(\mathbf{s}, \mathbf{a})$ can be calculated by defining the value of each action a, which is described as

$$q_\pi(\mathbf{s}, \mathbf{a}) = E_\pi\left[\sum_{k=0}^{\infty} \gamma^k R_{t+k+1} | S_t = \mathbf{s}, A_t = \mathbf{a}\right]. \tag{32}$$

Bellman optimal recursive equations of the optimal state value function $v * \mathbf{s}$ and the optimal action value function $q * \mathbf{s}$ can be calculated by introducing Markov property into (31) and (32), which can be shown as follows:

$$\begin{aligned} v*(s) &= \max_a R_s^a + \gamma \sum_{s_t \in S} p_{ss'}^a v*(s'), \\ q_\pi(\mathbf{s}, \mathbf{a}) &= R_s^a + \gamma \sum_{s' \in S} p_{ss'}^a \max_a q*(s', a'), \end{aligned} \tag{33}$$

where $\mathbf{s}'$ and $\mathbf{a}'$ are the state and action of the next moment, respectively.

The optimal strategy derived by maximizing the above functions can be represented as

$$\pi*(\mathbf{a}|\mathbf{s}) = \begin{cases} 1, & if\left(\mathbf{a} = \arg\max_{a \in A} q*(\mathbf{s}, \mathbf{a})\right), \\ 0, & else. \end{cases} \tag{34}$$

The function can be calculated by Q-learning algorithm, and the algorithm process is shown in Algorithm 1.

In Algorithm 1, $\mathbf{s}_T$ is the termination state in the fifth row. The current value function of the subsequent state estimation is used to update the optimal action function in the seventh row. In order to enhance the diversity of the exploration ability of the algorithm, the specific formula is shown as

$$\pi(\mathbf{a}|\mathbf{s}) = \begin{cases} 1 - \varepsilon + \dfrac{\varepsilon}{N(a)}, & \mathbf{a} = \arg\max_a q(\mathbf{s}, \mathbf{a}), \\ \dfrac{\varepsilon}{N(a)}, & \mathbf{a} \neq \arg\max_a q(\mathbf{s}, \mathbf{a}), \end{cases} \tag{35}$$

where $N(\boldsymbol{a})$ is the total number of actions, ε-greedy is the optimal action strategy taken based on 1-ε probability, and random action is the policy of ensuring the possibility of being selected for each action according to the probability of ε.

4. SUMO/Python Simulation and Analysis

In this section, we will simulate and analyze the proposed MSTTOM through the SUMO/Python-based platform to verify the feasibility and effectiveness of the scheme. Meanwhile, the optimal level of mobility at the signal intersection will be guaranteed in the experiment.

Q-learning algorithm
(1) Initialize $q(\mathbf{s}, \mathbf{a})$;
(2) While $(\mathbf{s}_t = \mathbf{s}_T)$
(3) {Select the initial state $\boldsymbol{s}_0$ and action $\boldsymbol{a}_0$ according to the ε-greedy strategy;
(4) While $(\mathbf{s}_t = \mathbf{s}_T)$
(5) {Select the action $\mathbf{a}_t$ the state $\mathbf{s}_t$ according to the ε-greedy strategy, get reward $\mathbf{r}_t$ and the next state $\boldsymbol{s}_{t+1}$;
(6) $q(\mathbf{s}_t, \mathbf{a}_t) \leftarrow q(\mathbf{s}_t, \mathbf{a}_t) + \mathbf{a}(\mathbf{r}_{t+1} + \gamma \max_{\mathbf{a}} q(\mathbf{s}_{t+1}, \mathbf{a}) - q(\mathbf{s}_t, \mathbf{a}_t))$;
(7) $\mathbf{s}_t = \mathbf{s}_{t+1}$; } }
(8) Get the optimal strategy $\pi(\mathbf{s}) = \arg\max_{\mathbf{a}} q(\mathbf{s}, \mathbf{a})$

Algorithm 1: Q-learning algorithm.

4.1. Experiment Platform Based on SUMO. SUMO is microscopic traffic simulation software [20]. The simulation of SUMO is discrete in time and continuous in space, and the location of each vehicle is described internally. In SUMO, the vehicle model is collision free, so that the variation caused by incomplete model is not allowed to appear in the simulation. SUMO allocates appropriate routes to vehicles considering different traffic demands through Dijkstra algorithm. The structure of SUMO map is shown in Figure 7.

4.2. Experimental Scheme. In the paper, the Netedit of SUMO is used to carry out the multilane experimental scenario based on Figure 1, and the simulation scenario is shown in Figure 8. The intersection is a typical cross intersection, and the traffic light is set as a typical four-phase signal light. Due to the similar spatial characteristics of each section, the 4-lane section from west to east is selected for the experiment.

In the simulation process, the benchmark scheme in the software, the glidepath prototype application (GPPA) scheme [21], and the MSTTOM scheme proposed in this paper are used to simulate and compare the performance of traffic flow conditions with various vehicle saturation 0.6, 0.8, and 1.0. Vehicles simulation diagram is shown in Figure 9.

The three schemes compared in this paper are defined as follows:

(i) The benchmark scheme: in this scheme, the traditional human driving vehicle model in SUMO software is adopted, which means that there is no controlled vehicle and no network communication. Therefore, the driving situation of vehicles under the current traditional driving habits can be simulated in this scenario.

(ii) GPPA scheme: GPPA driving optimization scheme developed by the Federal Highway Administration (FHWA) has been tested and verified. In this scheme, all vehicles in the traffic flow are CVs and are controlled by the optimized system of GPPA.

(iii) MSTTOM scheme: all vehicles in this scheme are CVs, and MSTTOM was applied to all vehicles in this paper. Compared with GPPA scheme, there are the advantages of strong stability and fast calculation efficiency in MSTTOM. Meanwhile, this scheme is adaptive in the complex multilane and multivehicle scenario.

Simulation conditions and parameter settings for these three schemes are shown in Table 1. Meanwhile, car-following state is simulated by Krauss car-following model [22].

In order to eliminate the influence of unrelated factors in the scenario, the simulation settings in SUMO are simplified by considering the following conditions:

(i) In the simulation environment, there are the same model, size, and kinematic characteristics with all vehicles.

(ii) There is no special weather effect in the simulation environment, and the road adhesion coefficient remains constant.

(iii) The roads are straight in the simulation environment. There are no ramps, nonmotorized vehicular lanes, or parking spaces, which lead to vehicles entering or exiting.

(iv) There is no inclination change in the road section, which means that the vehicle will not travel uphill or downhill.

(v) The arrival probability of vehicles in the simulation environment is stochastic and obeys the Poisson distribution.

The simulation process based on SUMO is shown in Figure 10. It can be seen that the red vehicle from the west to the east attempts to go straight through the intersection within the green duration from the rightmost lane. In this process, the red vehicle completes cooperative lane-changing with vehicles in the left lane through MSTTOM.

4.3. Result Analysis. Through the simulation of SUMO software, the output data of the vehicle can be exported and analyzed. The vehicular spatiotemporal trajectories on the left lane of the test road section are shown in Figure 11, where the spatiotemporal trajectory of the vehicle running on the right lane is denoted by the blue dotted line, and the spatiotemporal trajectory of the vehicle running on the left lane is represented by the red solid line. It is worth noting that the lane-changing vehicles can complete lane-changing quickly and safely

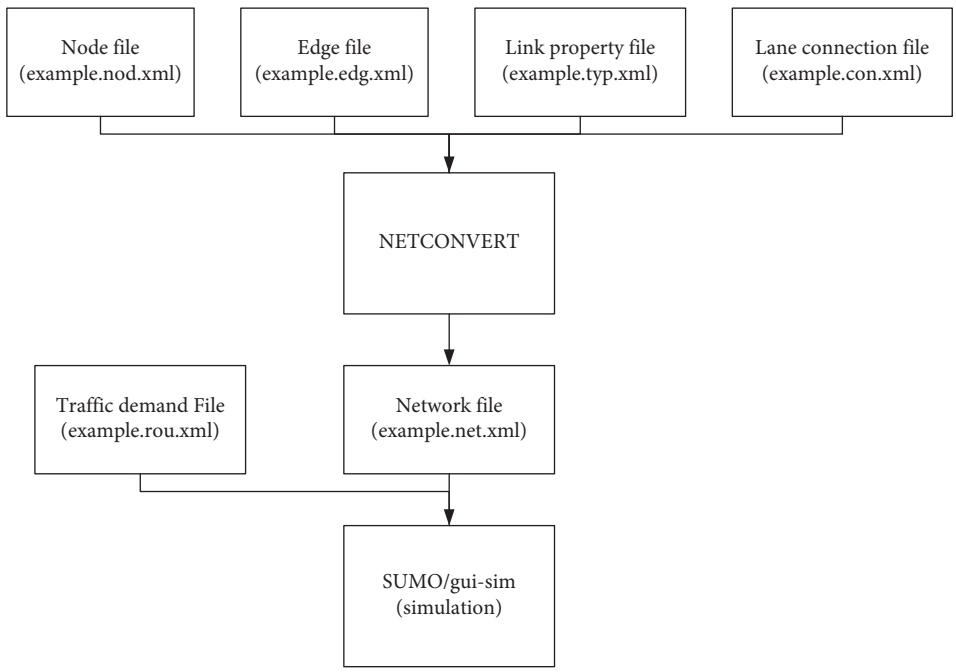

Figure 7: The structure of SUMO map.

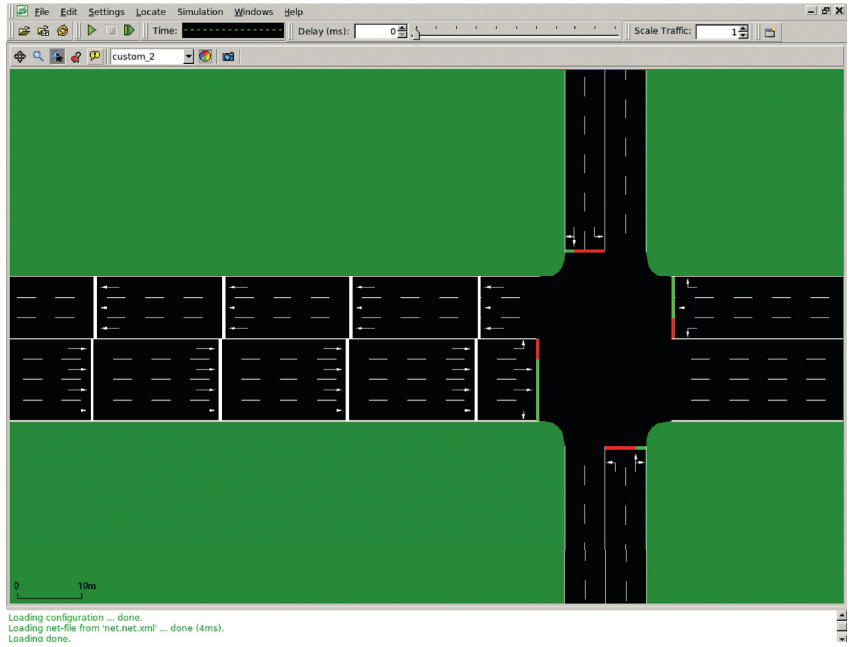

Figure 8: Diagrammatic sketch of simulation scenario.

under the optimized method. Once a vehicle requests the change of its lane, vehicles in the target lane can adjust the vehicle position and reserve the optimal safety gap for the vehicle requesting lane-changing. Under the environment of multilane signalized intersection, there is no sharp speed change when vehicles approach the intersection. Therefore, the efficiency of achieving the expected optimization of vehicular lane-changing can be proved for the vehicular cooperative optimization.

The headway and lost time at the stop line of intersection in the road network are analyzed in Figure 12, where the blue curve is the test statistical result of the left lane in the benchmark scheme, the green curve is the test statistical result of the left lane in GPPA scheme, and the red curve is the test statistical result of the left lane in MSTTOM scheme. The meaningless data of the first vehicle in the green and red phases in the experimental results are not included in the above statistics. The jumping part of the curve is the loss time

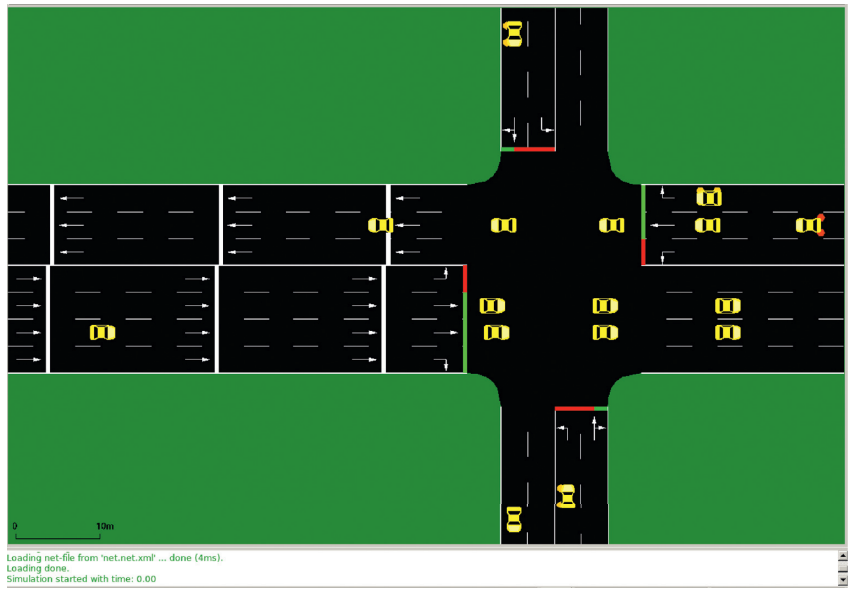

Figure 9: Diagrammatic sketch of vehicles simulation.

Table 1: Simulation conditions and parameter settings.

Parameters	Unit	Value
Distance from detector to intersection	(m)	200
Minimum headway at rest	(m)	2
Vehicle length	(m)	4.5
Vehicle width	(m)	1.8
Vehicle height	(m)	1.5
Lane width	(m)	3.5
Signal cycle duration	(s)	60
Green light duration	(s)	12
Red light duration	(s)	45
Yellow light duration	(s)	3
Saturated traffic flow rate	(Veh/h/lane)	1800
Maximum vehicle speed	(km/h)	60
Minimum vehicle speed	(km/h)	0
Maximum vehicle acceleration	(m/s2)	2.6
Maximum vehicle deceleration	(m/s2)	−4
Maximum vehicle lateral acceleration	(m/s2)	2
Maximum vehicle lateral deceleration	(m/s2)	−2
Maximum vehicle jerk	(m/s3)	10
Weight coefficient w_1	—	100
Weight coefficient w_2	—	50
Weight coefficient w_3	—	10
Weight coefficient w_4	—	200
Weight coefficient w_5	—	1
Weight coefficient w_6	—	5

of the first vehicle at the beginning of the green light or the lost time of the headway of the following vehicles. Through observation, it can be found that the headway of vehicles can be effectively reduced, the number of vehicles passing through the intersection stop line in a unit time is increased, and the saturation flow rate at the intersection is improved in MSTTOM scheme. In the process of GPPA scheme, some vehicles are affected by vehicular lane-changing, which results in a significant increase in the headway and raise in the green light loss time. Under MSTTOM scheme, the headway of vehicles at the intersection is significantly reduced, and the saturated flow rate at the intersection is increased. According to the traffic control characteristics of signalized intersections, the increase of effective green time and saturation flow rate will directly lead to an increase in the number of vehicles passing through the stop line at the intersection, which means that the throughput of the intersection will be improved.

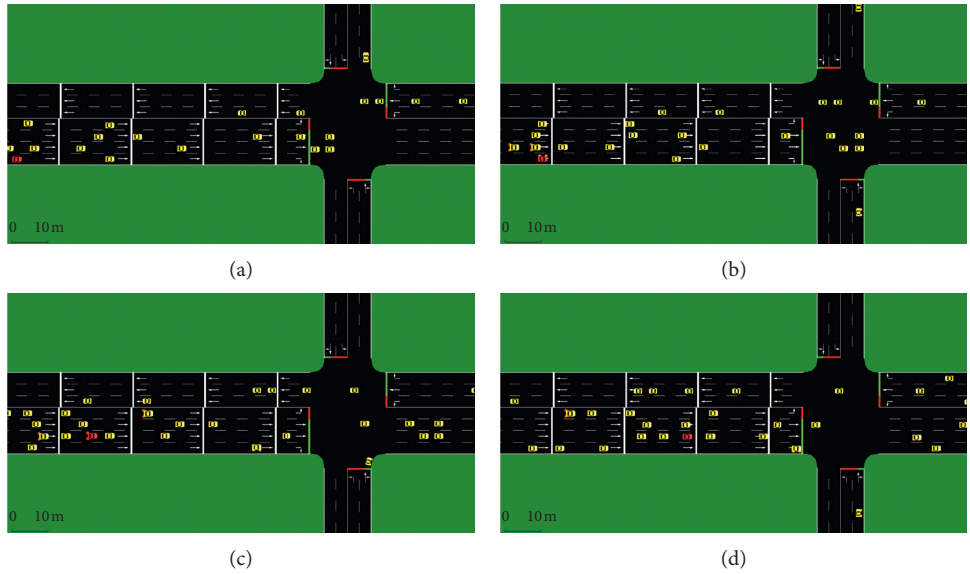

Figure 10: Part of the simulation process based on SUMO.

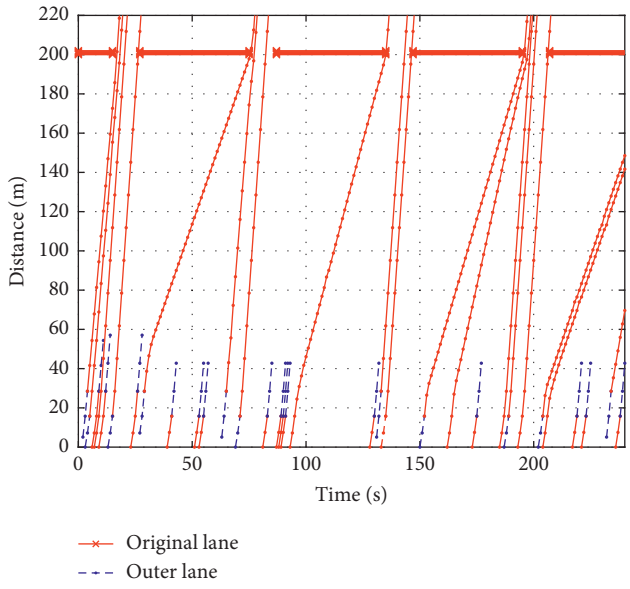

Figure 11: Spatiotemporal trajectories of left lane.

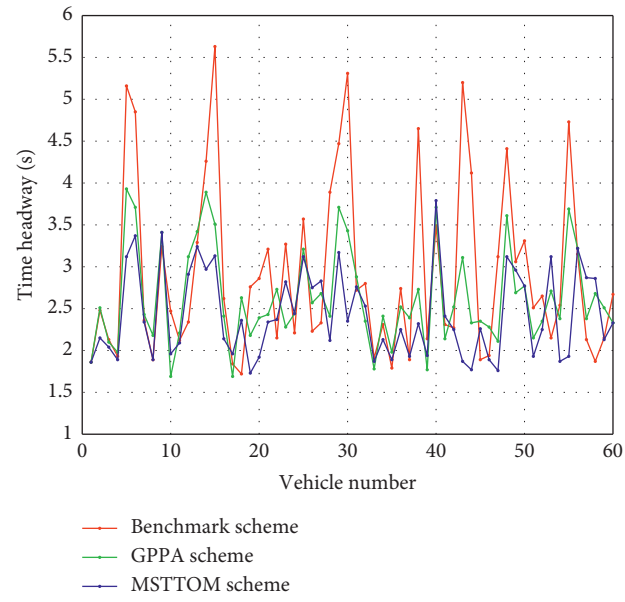

Figure 12: Headway variation under different schemes.

The vehicle fuel efficiency and corresponding profit of the whole system under MSTTOM are analyzed in Figure 13. The results of T-test show that there is a significant statistical difference in the vehicle fuel efficiency data between the MSTTOM scheme and the benchmark scheme. Through observation, it can be seen that the use of MSTTOM can effectively improve the vehicle fuel efficiency and reduce the vehicle fuel consumption.

After calculation, the vehicle fuel consumption profit is shown in Figure 14. In the case of different vehicle saturation, there is a significant fuel efficiency benefit in GPPA scheme and MSTTOM scheme. Comparing GPPA scheme with the scheme of optimization method proposed in this paper, the advantages of MSTTOM scheme in improving traffic mobility, enhancing vehicle fuel efficiency, and reducing pollutants emissions are obvious.

In MSTTOM scheme, the system calculation time analysis under different iteration time steps and optimization time spans is demonstrated in Figure 15. The maximum calculation time is up to 0.93 when the optimization time span is 50 seconds, and the iteration time step is 0.2 seconds. In the simulation process, the optimization time spans of all CVs are less than 50 seconds, and each iteration time step is greater than 0.2 seconds. Therefore, the calculation time of

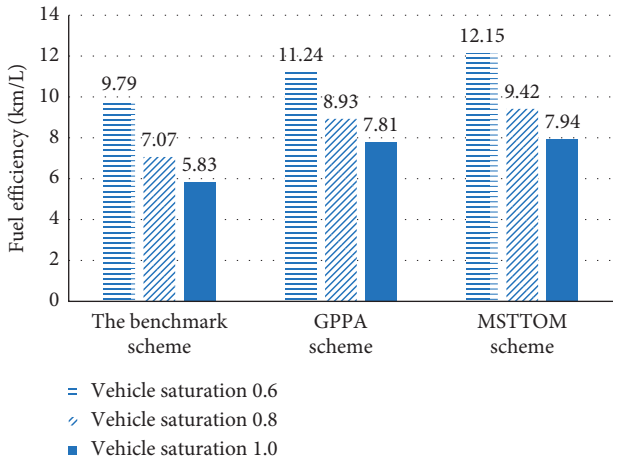

Figure 13: Fuel efficiency under different schemes.

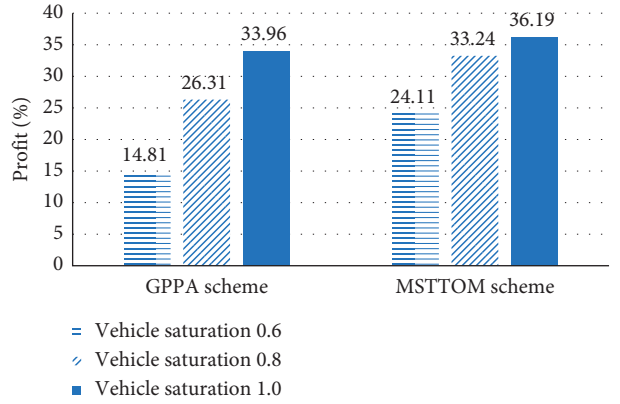

Figure 14: Vehicle fuel consumption profit under different schemes.

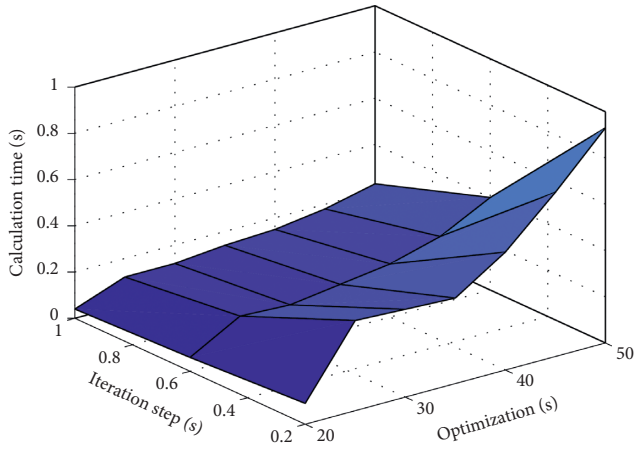

Figure 15: System calculation time under different optimization parameters.

the system is less than 1 second; that is, the effective performance of the system time meets the requirements of real-time optimization.

The objectives of ensuring the optimal mobility of vehicles at signalized intersections, enhancing vehicle fuel efficiency, and reducing pollutants emissions can be achieved in MSTTOM scheme. Compared with the existing GPPA algorithm, the strengths of MSTTOM are as follows:

(i) The function of multilane cooperative lane-changing strategy under the condition of random traffic flow is well realized in MSTTOM scheme.

(ii) Compared with the benchmark scheme, the mobility of vehicles within the road section is improved, the vehicle fuel efficiency is enhanced by 32%, and the emissions of pollutants are reduced by 17% in MSTTOM scheme.

(iii) Compared with the advanced GPPA scheme, there is a 24% reduction in the vehicle fuel consumption in MSTTOM scheme.

(iv) The traffic fluctuation caused by the intersection signal control is smooth and the traffic flow in the road section is more reasonable in MSTTOM scheme.

(v) For the randomness in the traffic process, the MSTTOM scheme shows its superiority in robustness than other existing schemes.

(vi) The calculation time in MSTTOM scheme is less than 1 second, and the distribution is mainly concentrated in 0.3 seconds to 0.7 seconds, which satisfies the requirements of real-time optimization.

5. Conclusions

This paper proposes a new scheme, MSTTOM, to ease traffic pressure and reduce traffic congestion in multilane road sections. The problem of low traffic efficiency at the multilane intersections is studied and analyzed in this paper. Four stages of work, namely, literature summary, scenario and structure introduction, method optimization design and experimental validation, and optimization objects determination, are conducted. The research results and innovations are as follows:

(i) A vehicular lane-changing method based on V2X is proposed. Firstly, the lane-changing environment information is analyzed to classify and define the potential threat vehicles in the driving environment. Secondly, the lane-changing behaviors of potential threat vehicles are analyzed, and conflict detection is carried out to determine the priority order in the lane-changing process. Then, lane-changing gap and target cooperative vehicles are determined and declared. Finally, the spatiotemporal trajectories of related vehicles are updated. The vehicular cooperative lane-changing strategy lays a foundation for the reasonable planning of MSTTOM.

(ii) This paper designs a multilane spatiotemporal trajectory optimization method. Based on the optimal control theory, the state control models of CVs driven by Pontryagin's maximum principle are constructed. The cost function is formulated by continuous functional target completion and

optimal profit. The constraints in line with the actual situation of the vehicle are also established. Finally, the trajectories data are optimized by Q-learning algorithm to achieve the real-time optimization.

(iii) SUMO software is used to verify the feasibility and effectiveness of MSTTOM by comparing it with GPPA scheme of FHWA in the United States. The experimental results demonstrate that MSTTOM can effectively optimize the traffic flow, improve the vehicle fuel efficiency, reduce pollutants emissions, and improve the traffic efficiency of vehicles at intersections.

Data Availability

All data generated or analyzed during this study are included in this article.

Conflicts of Interest

The authors declare that there are no conflicts of interest regarding the publication of this paper.

Acknowledgments

This work was supported by National Key R&D Program of China (Grant no. 2018YFB1600500) and Beijing Nova Program (Grant no. Z181100006218076).

References

[1] P. Reina and S. Ahn, "Lane flow distribution of congested traffic on three-lane freeways," *International Journal of Transportation Science and Technology*, vol. 9, no. 1, pp. 1–13, 2020.

[2] E. Suryani, R. A. Hendrawan, P. F. EAdipraja, A. Wibisono, and L. P. Dewi, "Modelling reliability of transportation systems to reduce traffic congestion," in *Proccedings of the Journal of Physics: Conference Series*, vol. 1196, no. 1, Article ID 12029, Palembang, Indonesia, November 2019.

[3] M. Tajalli and A. Hajbabaie, "Distributed optimization and coordination algorithms for dynamic speed optimization of connected and autonomous vehicles in urban street networks," *Transportation Research Part C: Emerging Technologies*, vol. 95, pp. 497–515, 2018.

[4] E. Grumert and A. Tapani, "Impacts of a cooperative variable speed limit system," *Procedia-Social and Behavioral Sciences*, vol. 43, pp. 595–606, 2012.

[5] Y. Jo, H. Choi, S. Jeon, and I. Jung, "Variable speed limit to improve safety near traffic congestion on urban freeways," *International Journal of Fuzzy Systems*, vol. 14, no. 2, 2012.

[6] Y. Fang and Z. Y. Guo, "Research on the method of dynamic speed limit on expressway under complex climate based on pavement skid-resistant performance," *Advanced Materials Research*, vol. 2478, 2013.

[7] F. Zhu and S. V. Ukkusuri, "Accounting for dynamic speed limit control in a stochastic traffic environment: a reinforcement learning approach," *Transportation Research Part C Emerging Technologies*, vol. 41, pp. 30–47, 2014.

[8] M. Aldana-Muñoz, E. Maeso-González, and A. García-Rodríguez, "Contributions of eco-driving on traffic safety," *Securitas Vialis*, vol. 7, pp. 1–3, 2016.

[9] J. F. Wang, C. C. Li, J. R. Lv, and X. D. Yan, "Speed guidance model during the green phase based on a connected vehicle," *Simulation*, vol. 92, no. 10, pp. 899–905, 2016.

[10] Y. Wei, C. Avcı, J. Liu et al., "Dynamic programming-based multi-vehicle longitudinal trajectory optimization with simplified car following models," *Transportation Research Part B Methodological*, vol. 106, pp. 102–129, 2017.

[11] R. De Mello and R. D. Chiodi, "A safe speed guidance model for highways," *International Journal of Injury Control and Safety Promotion*, vol. 54, no. 4, pp. 408–415, 2018.

[12] X. Liang, S. I. Guler, and V. V. Gayah, "Joint optimization of signal phasing and timing and vehicle speed guidance in a connected and autonomous vehicle environment," *Transportation Research Record: Journal of the Transportation Research Board*, vol. 2674, no. 4, pp. 70–83, 2019.

[13] P. Wang, Y. Jiang, L. Xiao, Y. Zhao, and Y. Li, "A joint control model for connected vehicle platoon and arterial signal coordination," *Journal of Intelligent Transportation Systems*, vol. 24, no. 1, pp. 81–92, 2020.

[14] P. Wang, H. Deng, J. Zhang, and M. Zhang, "Real-time urban regional route planning model for connected vehicles based on V2X communication," *Journal of Transport and Land Use*, vol. 13, no. 1, pp. 517–538, 2020.

[15] A. Mirheli, M. Tajalli, L. Hajibabai, and A. Hajbabaie, "A consensus-based distributed trajectory control in a signal-free intersection," *Transportation Research Part C: Emerging Technologies*, vol. 100, pp. 161–176, 2019.

[16] P. Wang, P. Li, F. R. Chowdhury, L. Zhang, and X. Zhou, "A mixed integer programming formulation and scalable solution algorithms for traffic control coordination across multiple intersections based on vehicle trajectories," *Transportation Research Part B: Methodological*.vol. 134, pp. 266–304, 2020.

[17] M. A. Benloucif, J. Popieul, and C. Sentouh, "F for multi-level cooperation and dynamic authority management in an Automated Driving System-a case study on lane change cooperation," *IFAC PapersOnLine*, vol. 49, no. 19, pp. 615–620, 2016.

[18] A. Hongil and J. Jae-Il, "Design of a cooperative lane change protocol for a connected and automated vehicle based on an estimation of the communication delay," *Sensors*, vol. 18, no. 10, p. 3499, 2018.

[19] L. Li, J. Gan, K. Zhou, X. Qu, and B. Ran, "A novel lane-changing model of connected and automated vehicles: using the safety potential field theory," *Physica A: Statistical Mechanics and Its Applications*, vol. 559, Article ID 125039, 2020.

[20] J. Zambrano-Martinez, C. Calafate, D. Soler, J. C. Cano, and P. Manzoni, "Modeling and characterization of traffic flows in urban environments," *Sensors*, vol. 18, no. 7, 2018.

[21] O. D. Altan, G. Wu, M. J. Barth, K. Boriboonsomsin, and J. A. Stark, "GlidePath: eco-friendly automated approach and departure at signalized intersections," *IEEE Trans. Intelligent Vehicles*, vol. 2, no. 4, pp. 266–277, 2017.

[22] V. Kanagaraj, G. Asaithambi, C. N. Kumar, K. K. Srinivasan, and R. Sivanandan, "Evaluation of different vehicle following models under mixed traffic conditions," *Procedia-Social and Behavioral Sciences*, vol. 104, pp. 390–401, 2013.